Construction and Building Materials 247 (2020) 118641

Contents lists available at ScienceDirect

Construction and Building Materials

journal homepage: www.elsevier.com/locate/conbuildmat

# Correlation between pore structure, compressive strength and thermal conductivity of porous metakaolin geopolymer

Nur Ain Jaya [a], Liew Yun-Ming [a,*], Heah Cheng-Yong [a,b], Mohd Mustafa Al Bakri Abdullah [a], Kamarudin Hussin [a,b]

[a] Center of Excellence Geopolymer and Green Technology (CeGeoGTech), School of Materials Engineering, Universiti Malaysia Perlis (UniMAP), Kangar, 01000 Perlis, Malaysia
[b] Faculty of Engineering Technology, Universiti Malaysia Perlis (UniMAP), Sungai Chuchuh, Padang Besar, 02100 Perlis, Malaysia

## HIGHLIGHTS

- Thermal conductivity of neat geopolymer was affected greatly by MK/AA ratio.
- Combined foam and surfactant generated smaller and narrower pore size distribution.
- Effect of surfactant as pore stabilizer was prominent at low foaming agent content.
- Pore volume and connectivity govern the thermal conductivity of porous geopolymer.
- Geopolymer foam could be applied as Class II – structural and insulating materials.

## ARTICLE INFO

*Article history:*
Received 21 October 2019
Received in revised form 3 February 2020
Accepted 1 March 2020
Available online 6 March 2020

*Keywords:*
Geopolymer
Metakaolin
Porous
Pore
Foam
Surfactant

## ABSTRACT

This paper investigates the effect of mixing parameters (that are, alkali concentration, AA ratio, and MK/AA ratio) on the thermal conductivity of metakaolin geopolymers. The combination effect of foaming agent ($H_2O_2$) and surfactant (Tween 80) on the physical properties, compressive strength, and pore characteristic was also elucidated. Results showed that metakaolin geopolymer with maximum compressive strength of 33 MPa, bulk density of 1680 kg/m$^3$, porosity of 18% and thermal conductivity of 0.40 W/mK were achieved with alkali concentration of 10 M, AA ratio of 1.0 and MK/AA ratio of 0.8. Gradation analysis demonstrated that AA ratio was the strength determining factor. Whilst, thermal conductivity was dependent on the MK/AA ratio. Adding $H_2O_2$ and surfactant produced geopolymer foam with acceptable compressive strength (0.4–6 MPa). The geopolymer foam had bulk density of 471–1212 kg/m$^3$, porosity of 36–86% and thermal conductivity of 0.11–0.30 W/mK. Pore structure, size, and distribution were governed by $H_2O_2$ and surfactant dosages that have a great impact on the compressive strength. Narrower pore distribution and smaller pore diameter were achieved when both foaming agent and surfactant were used instead of foaming agent alone. The pore size and distribution varied to a greater extent with varying $H_2O_2$ contents. Surfactant illustrated distinct pore stabilizing effect at low $H_2O_2$ (<0.75 wt%) which diminished at high $H_2O_2$ content. In terms of thermal conductivity, even with increasing porosity at high $H_2O_2$ and surfactant content, the thermal conductivity did not show substantial reduction due to the interconnected pores as a result of pore coalescence.



## 1. Introduction

Geopolymer has received significant attention in recent years. The important contribution of geopolymer is in the construction industry wherein geopolymer serves as an alternative binder for mortars and concretes [1]. Geopolymer is produced through geopolymerisation reaction of aluminosilicate materials (for instance, kaolin, metakaolin, and Class F fly ash) and alkali activator (usually a mixture of alkali hydroxide and alkali silicate). Geopolymerisation involves the dissolution and polycondensation process that occurs at room temperature or slightly higher temperature producing Si-O-Al polymeric framework with $SiO_4$ and $AlO_4$ linked tetrahedrally by sharing oxygen atom. Metakaolin has been extensively used in geopolymer formation due to its high reactivity [2]. Geopolymer properties are strongly dependent on the synthesis parameters such as aluminosilicates' proportion; alkali activator's types, concentration and proportion; and curing condition

* Corresponding author.
*E-mail address:* ymliew@unimap.edu.my (L. Yun-Ming).

https://doi.org/10.1016/j.conbuildmat.2020.118641
0950-0618/

[3]. These factors determine the dissolution ability, kinetics of geopolymerisation [1], viscosity of geopolymer paste [4], compactness of final product [5] and subsequently the mechanical performance of geopolymer. The variation in the reaction and final products led to the difference in the thermal conductivity of geopolymers.

The development and application of geopolymers in thermal insulation of buildings are also one of the research interest. Thermal conductivity (λ) is an important measurement when considering the thermal insulating properties. Thermal conductivity measures the heat transfer in a material whereby a lower λ value indicates better insulation [6]. In general, geopolymer has low λ (<0.70 W/mK) [7] which is approximately 50% lower than Portland cement (PC) materials [8,9]. The thermal insulating properties could be further improved by introducing pores or voids in geopolymer matrix. Pores are usually generated by chemical (e.g. foaming agents such as Al powder [10], silica fume [11], hydrogen peroxide [12], sodium hypochlorite [13] and sodium perborate [14]) or mechanical foaming (e.g. preformed foam [15]). In this study, metakaolin geopolymer foam was prepared by introducing hydrogen peroxide ($H_2O_2$) as the foaming agent. $H_2O_2$ reacts in basic media generating water and oxygen gas as shown in Eq. (1) [16]. Pores are introduced by the gas formed in the geopolymer matrix.

$$H_2O_2 \rightarrow H_2O + 1/2O_2 \quad (1)$$

Geopolymer foam is usually termed as foam concrete which defined as cellular concrete having high-voids space, with or without aggregates [17]. Based on the functional classification of International Union of Laboratories and Experts in Construction Materials, Systems and Structures (RILEM) [18], lightweight concretes could be classified into Class I, II and III based on their compressive strength, density and thermal conductivity values. Class I is structural lightweight concrete with density of 1440–1840 kg/m$^3$, compressive strength >17 MPa and λ of 0.4–0.7 W/mK. On the other hand, Class II is structural and insulating lightweight concrete with density of 800–1400 kg/m$^3$, compressive strength of 3.4–17 MPa, and λ of 0.22–0.43 W/mK. Class III is defined as insulating lightweight concrete with low density (240–800 kg/m$^3$), compressive strength (0.7–3.4 MPa and λ (0.065–0.22 W/mK).

Porous geopolymer can have density lower than 600 kg/m$^3$ with a low λ of 0.1 W/mK [19]. According to Samson et al. [20], the porous structure was governed by the foaming agent and surfactant contents which consequently affecting the density and mechanical strength. The degree of porosity controls the mechanical strength and thermal conductivity of the geopolymer foam. The amount of porosity in the range of 50–95% was required in order to achieve lightweight and thermal insulating properties [21]. Based on Zhang et al. [22], geopolymer foam usually possesses compressive strength <10 MPa with density range of 360–1400 kg/m$^3$. Ducman & Korat [23] reported compressive strength of 3.3 MPa and 3.7 MPa, density of 640–740 kg/m$^3$ and 610–1000 kg/m$^3$ and porosity of 59% and 48% for fly ash geopolymers foamed with Al powder and $H_2O_2$, respectively. Based on them, geopolymer foamed with $H_2O_2$ has finer pore distribution than that using Al powder.

The pore dispersion and morphology of the final foam product have strong impact on the mechanical strength and the effective thermal insulation [11]. Masi et al. [16] obtained compressive strength of 1.7–4.6 MPa for fly ash geopolymer foamed with $H_2O_2$ and with the addition of surfactant (Sika Lightcrete). The macropores were reported in the range of 50–1000 μm. According to Kamseu et al. [24], metakaolin geopolymer foam was reported having λ of 0.15–0.40 W/mK with porosity of 30–70%.

In this work, metakaolin geopolymer and geopolymer foam were prepared. The optimization of mixing parameters (NaOH concentration, MK/AA ratio, and AA ratios) of metakaolin geopolymer was investigated as mixing formulation was known crucially affecting the physical and mechanical properties of geopolymer. Their effect on thermal conductivity was also studied. In addition, the joint effect of foaming agent and surfactant on geopolymer foam in terms of physical properties, mechanical strength, pore size, pore distribution, and thermal conductivity was analysed. In previous literature [9,23,25,26], studies mostly focused on the pore morphology of geopolymer foam with very little emphasis on the effect of pore size and distribution on the mechanical strength and thermal conductivity. Despite there was an investigation on pore size distribution, solely foaming agent was used in the formation of geopolymer. For instance, Hajimohammadi et al. [27] and Cui et al. [28] investigated the pore size distribution of one-part geopolymer foamed with preformed foam and fly ash geopolymer foamed with $H_2O_2$, respectively. Beghoura et al. [29] performed the pore size distribution by image analysis on geopolymer based on waste mud, waste glass and metakaolin foamed with Al powder. The combination effect of foaming agent and surfactant on pore properties was scarce. Therefore, this paper provides a comprehensive study of mixing parameter optimization and its effect on thermal conductivity. The joint effect and correlation of foaming agent and surfactant on geopolymer foam in terms of physical properties, mechanical strength, pore characteristic, and thermal conductivity was elucidated.

## 2. Experimental work

### 2.1. Materials

Metakaolin, a highly reactive mineral clay, was used as the precursor material in this work. The metakaolin was obtained by calcining kaolin at 850 °C for 6 h in the laboratory furnace which selected based on the optimum calcination profile obtained by Wan et al. [30]. The chemical composition of metakaolin determined by X-ray fluorescence (XRF) spectrometer is shown in Table 1. The metakaolin comprised of total $SiO_2$ and $Al_2O_3$ contents of 94.3%. Fig. 1 reveals the microstructure of metakaolin. The metakaolin presented a flake-like structure.

The alkaline activator solution was a mixture of sodium hydroxide (NaOH) and liquid sodium silicate ($Na_2SiO_3$). The ratio of $Na_2SiO_3$/NaOH was termed activator (AA) ratio. The NaOH powder has 99% purity with a density of 2.13 g/cm$^3$, while the liquid $Na_2SiO_3$ contains 30.1% $SiO_2$, 9.4% $Na_2O$ and 60.5% $H_2O$ with a density of 2.4 g/cm$^3$. The NaOH solution of the desired molar concentration was prepared and allowed to cool down at room temperature.

A 3 wt% hydrogen peroxide solution (diluted from 30 wt% $H_2O_2$, Sigma-Aldrich) was selected as the foaming agent. Tween 80 (polyethylene glycolsorbitan monooleate, VWR BDH Prolabo, Briare, France) was added as surfactant.

**Table 1**
Chemical composition of metakaolin as determined by XRF analysis.

| Chemical compound | Weight Percent (wt.%) |
|---|---|
| $SiO_2$ | 55.7 |
| $Al_2O_3$ | 38.6 |
| $Fe_2O_3$ | 2.03 |
| $TiO_2$ | 0.78 |
| CuO | 0.03 |
| $ZrO_2$ | 0.04 |
| $K_2O$ | 2.43 |
| $MnO_2$ | 0.04 |
| Others | 0.38 |

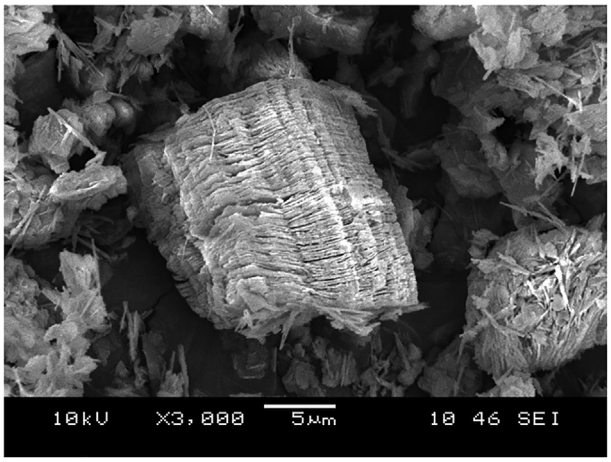


**Fig. 1.** SEM micrograph of metakaolin.

### 2.2. Preparation and optimization of metakaolin geopolymer

In the preparation of metakaolin geopolymer, metakaolin was mixed with alkali activator for 5 min by using a mechanical mixer to form a homogenous slurry. The fresh geopolymer paste was poured into high-density polyethylene (HDPE) mould with dimension of 50 mm × 50 mm × 50 mm. The moulded samples were vibrated for 2 min on the vibration table to remove entrained air and sealed with a thin film to prevent moisture loss. The geopolymer paste was left to cure at room temperature (29 °C) for 24 h and subsequently placed in an oven at 60 °C for another 24 h. Pre-curing at room temperature before curing in the oven was performed as it was beneficial for strength development [31,32]. After curing, the samples were demoulded and kept under room temperature until the day of testing. The NaOH concentration, metakaolin/activator (MK/AA) ratio, and AA ratio were varied as displayed in Table 2. The optimum mixing parameter was selected based on the highest compressive strength.

### 2.3. Preparation of metakaolin geopolymer foam

The metakaolin geopolymer paste was prepared as the steps aforementioned with NaOH concentration of 10 M, MK/AA ratio of 0.80 and AA ratio of 1 (based on optimum compressive strength in Section 2.2). Then, the surfactant was added into the paste at 500 rpm for 3 min followed by $H_2O_2$ at 500 rpm for 1 min. The dosage of surfactant was varied from 1, 3 and 5 wt% while $H_2O_2$ dosage was varied from 0.25, 0.50, 0.75, 1.00 and 1.25 wt%. The metakaolin geopolymer foams were moulded and cured at room temperature for 24 h, followed by 60 °C for another 24 h. After the curing process, the samples were kept under room temperature until the day of testing. Fig. 2 presents the schematic experimental procedure to produce an optimized geopolymer and geopolymer foam.

**Table 2**
Mixing parameters of metakaolin geopolymers in order to investigate the optimum formulation.

| Investigated Parameter | NaOH concentration | AA Ratio | MK/AA Ratio |
|---|---|---|---|
| NaOH | | Concentration | 6 M, 8 M, 10 M, 12 M and 14 M |
| 0.24 | 0.80 | | |
| AA Ratio | 10 M | 0.20, 0.24, 0.28, 0.30, 0.32, 0.40, 0.60, 0.80, 1.00 and 1.20 | 0.80 |
| MK/AA Ratio | 10 M | 1.00 | 0.60, 0.70, 0.80, 0.90 and 1.00 |

### 2.4. Testing and analysis method

The true density of the metakaolin geopolymers and geopolymer foams was determined by the pycnometer (AccuPyc II 1340 Helium pycnometer, Micromeritics). The bulk density was measured by the geometric method. The total porosity of the geopolymers and geopolymer foams was obtained from the bulk density to the true density ratio with Eq. (2).

$$\text{Total Porosity}(\%) = \left(1 - \frac{\text{bulk density}}{\text{true density}}\right) \times 100\% \quad (2)$$

Compressive strength after 28 days was tested based on the ASTM C109 using Instron machines series 5569 Mechanical Tester. The sample's surfaces were polished flat and parallel before testing. Three samples were tested for each parameter to obtain the average compressive strength value.

Room-temperature thermal conductivity (λ) was measured using a KD2 Pro Thermal Properties Analyzer (Decagon Devices Inc) which utilized the transient line heat source method according to IEEE 442-1981 and ASTM D5334. The pre-calibration of sensor was done based on DB1175 before each measurement. At least 3 measurements were performed to ensure accuracy.

The morphology of metakaolin geopolymer and geopolymer foam was observed using the JEOL JSM-6460 LA model Scanning Electron Microscopy (SEM). The specimen was cut into small pieces and coated with platinum by using Auto Fine Coater (JEOL JFC 1600) before the examination. In order to obtain the average pore diameter and distribution, the SEM micrographs were analysed using Image J image analysis software. The values obtained from the image analysis were converted to three-dimensional values using the stereological equation in Eq. (3).

$$D_{sphere} = \frac{D_{circle}}{0.785} \quad (3)$$

where $D$ is the diameter of pore.

The crystalline phases of the geopolymer were identified using powder X-ray Diffraction (XRD) collected on XRD-600 Shimadzu X-ray diffractometer using CuKα radiation scanning from 2θ values

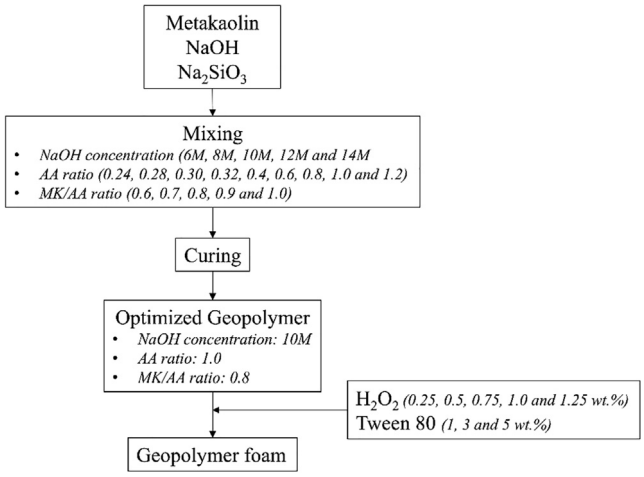


**Fig. 2.** Schematic experimental design to produce optimized geopolymer and geopolymer foam.

in the range of 10° to 80° generated at 30 mA and 40 kV with 0.02° 2θ steps. The specimen for analysis was prepared in powder form.

## 3. Results and discussion

### 3.1. Metakaolin geopolymer

#### 3.1.1. Bulk density and porosity

The bulk densities and porosities of metakaolin geopolymers are displayed in Fig. 3. In overall, the bulk density increased with increasing mixing parameters up to an optimal and then decreased. Yet, the variation of bulk density was marginal. The bulk density and porosity values complied with each other wherein metakaolin geopolymers with higher bulk density possessed lower porosity and vice versa. The metakaolin geopolymers exhibited bulk density between 1490 and 1680 kg/m$^3$. The bulk density values were comparable with those obtained by Rozek et al. [33] for fly ash geopolymer (1300–1600 kg/m$^3$) and Tippayasam et al. [34] for metakaolin geopolymer using potassium hydroxide (1720 kg/m$^3$).

Based on Fig. 3, the porosity value fell in the range of 18–30% which was lower than those recorded by Papa et al. [35] for metakaolin-zeolite geopolymers (34–49%). This might be attributed to the highly porous characteristic of zeolite [36]. On the other hand, Gorhan & Kurklu [37] obtained comparable porosity of 25–30% for fly ash geopolymers.

The changes of bulk density and porosity were comparatively more significant especially with varying MK/AA and AA ratios. Both ratios affected the fluidity of geopolymer mixture especially the MK/AA ratio. Lowering the MK/AA and AA ratios led to a highly workable mixture. A watery geopolymer mixture limited the contact between activator solution and aluminosilicate materials [38]. On due course, the dissolution ability was lower in order to optimize the polycondensation reaction. High liquid content in the geopolymer mixture in conjunction with less efficient dissolution and polycondensation created pores in the geopolymer matrix and thus high porosity [39]. This was due to moisture loss by evaporation and less formation of geopolymer products, respectively. On the other hand, increasing the MK/AA and AA ratios beyond optimum caused higher porosity as a result of the highly stiff mixture which restricted the proper consolidation of paste.

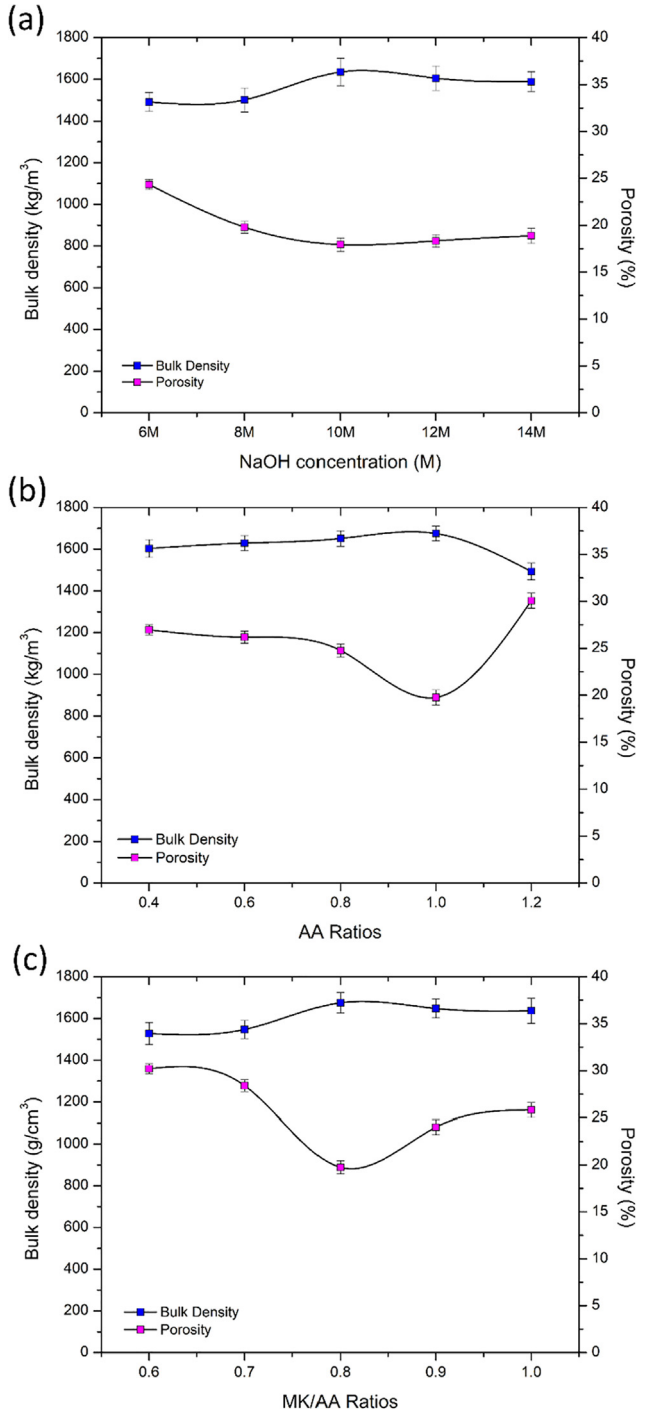


**Fig. 3.** Bulk densities and porosities of metakaolin geopolymers.

#### 3.1.2. Compressive strength

Mixing parameters are influential to the mechanical strength of metakaolin geopolymers. Referring to Fig. 4, the optimum

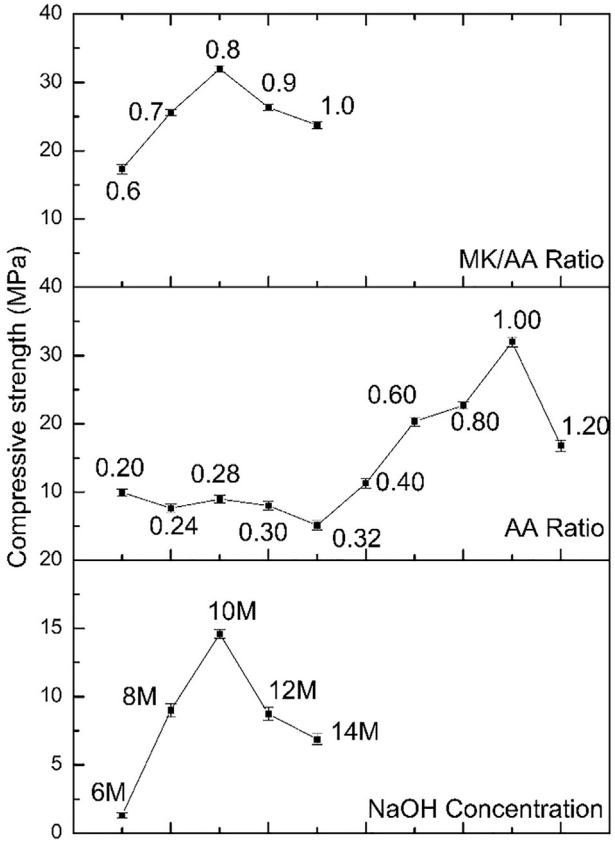


**Fig. 4.** Compressive strength of metakaolin geopolymers.

compressive strength of 33 MPa after 28 days was achieved with NaOH 10 M solution, AA ratio of 1.0, and MK/AA ratio of 0.8. Increasing each mixing parameter led to an increase of compressive strength up to an optimal and reduced beyond the optimal ratio. The compressive strength complied with the bulk density and porosity values recorded in Fig. 3.

During geopolymerization reaction, the alkali activator solution ensures optimum alkalinity for the dissolution of $Si^{4+}$ and $Al^{3+}$ to form $nM_2O{\cdot}Al_2O_3{\cdot}xSiO_2{\cdot}yH_2O$ matrix which then reorganizes and hardens to form dense rigid solid [40]. Gradation analysis (Table 3) showed that AA ratio was the key parameter affecting the mechanical properties of metakaolin geopolymers. The proportion of $Na_2SiO_3$ and NaOH in the activator solution was crucial as high AA ratio contributed more soluble Si, while low AA ratio contributed more $OH^-$ for dissolution purposes. The presence of soluble Si by $Na_2SiO_3$ could modify the reaction kinetics by enhancing the condensation process and thus improving the compressive strength [41].

Based on the previous studies [40,42,43], lower AA ratios in the range of 0.24–0.36 were mostly used. The optimum AA ratio was concluded at 0.24 by Wang et al. [42]. It had been proven in Fig. 4 that the metakaolin geopolymers produced in this range did not exhibit good compressive strength. Besides, it is worthwhile to highlight that in this study, a high AA ratio of 1.0 caused significant improvement of compressive strength which was approximately 200% increment with respect to strength with AA ratio in the range of 0.20–0.32. The result contradicted with Pelisser et al. [44] and Poowancum & Horpibulsuk [45] who reported that AA ratio of 1.0 produced porous and low strength geopolymer. In this study, further increase in the ratio led to 50% reduction of strength with respect to AA ratio of 1.0 as the mixture became viscous and difficult to consolidate which produced higher porosity (Fig. 3b) and consequently lower compressive strength (Fig. 4) [38,46]. The observation confirmed the conclusion made by Leong et al. [38].

On the other hand, increasing NaOH concentration facilitated the dissolution process of aluminosilicate and progress of geopolymerization. However, it did not further increase the compressive strength notwithstanding the higher NaOH concentration above 10 M. Excess $Na^+$ ions at high NaOH concentration may weaken the structure of geopolymer [47]. Moreover, as mentioned earlier, the MK/AA ratio mainly affected the workability of geopolymer mixture and thus the contact between the reacting materials [38]. This ratio also ensured that there was sufficient activator solution to dissolve the aluminosilicates. Thus, an extremely low or high MK/AA ratio was unlikely to improve the geopolymer formation.

**Table 3**
Gradation analysis based on compressive strength.

| Parameters | Value | Compressive strength (MPa) | Range* |
|---|---|---|---|
| NaOH concentration | 6 M | 1.29 | 13.31 |
| | 8 M | 9.00 | |
| | 10 M | 14.6 | |
| | 12 M | 8.74 | |
| | 14 M | 6.87 | |
| AA ratio | 0.4 | 11.29 | 20.70 |
| | 0.6 | 20.33 | |
| | 0.8 | 22.69 | |
| | 1.0 | 31.99 | |
| | 1.2 | 16.79 | |
| MK/AA ratio | 0.6 | 17.31 | 14.68 |
| | 0.7 | 25.60 | |
| | 0.8 | 31.99 | |
| | 0.9 | 26.37 | |
| | 1.0 | 23.73 | |

* Range = highest strength − lowest strength.

*3.1.3. Thermal conductivity (λ)*

The metakaolin geopolymer exhibited λ value in the range of 0.33–0.41 W/mK (Fig. 5). The λ value of metakaolin geopolymers followed the trend of bulk density (Fig. 3) and compressive strength (Fig. 4). The denser the geopolymer, the higher the compressive strength and thus higher the λ value [25]. Geopolymer can have a lower λ value by 50% compared to conventional PC material which has a λ value of 1.5 W/mK [8,9,48]. Geopolymerisation reaction produced amorphous and porous interconnected polysialates that provided the tortuous route for thermal gradient flow [49,50]. The amorphous structure of geopolymer restricted heat transfer. This was well-supported by Fongang et al. [8]. The poorer insulating properties (higher λ) of PC materials than geopolymer [15] were supposed due to the high content of chemically-bounded water [51] and lower porosity [52]. Chemically-bounded water provided a continuous gel structure for the transfer of heat, thus increased the λ value.

In addition, the λ value recorded in this study was lower by 54% than those recorded by Duxson et al. [53] for metakaolin geopolymer (0.78–0.82 W/mK). The higher λ value recorded by Duxson et al. [53] was most probably due to the presence of quartz (residual after calcination of kaolin) in the metakaolin geopolymers. Quartz had a high λ value of 6–11 W/mK [24] which thus tended to increase the overall λ value of the metakaolin geopolymers. Besides, the results obtained in this study showed that the λ value was comparable to metakaolin geopolymers developed by Kamseu et al. [54] (0.30–0.59 W/mK). However, Villaquiran-Caicedo et al. [55] obtained a lower λ value of 0.17–0.35 W/mK for metakaolin geopolymers using Si source from rice husk ash. This was due to the high open porosity which was related to the higher amount of hydration water and lower bulk density.

Pearson correlation coefficient study (Table 4) was performed to determine the correlation between λ, porosity, bulk density and compressive strength with varying mixing parameters. It is widely

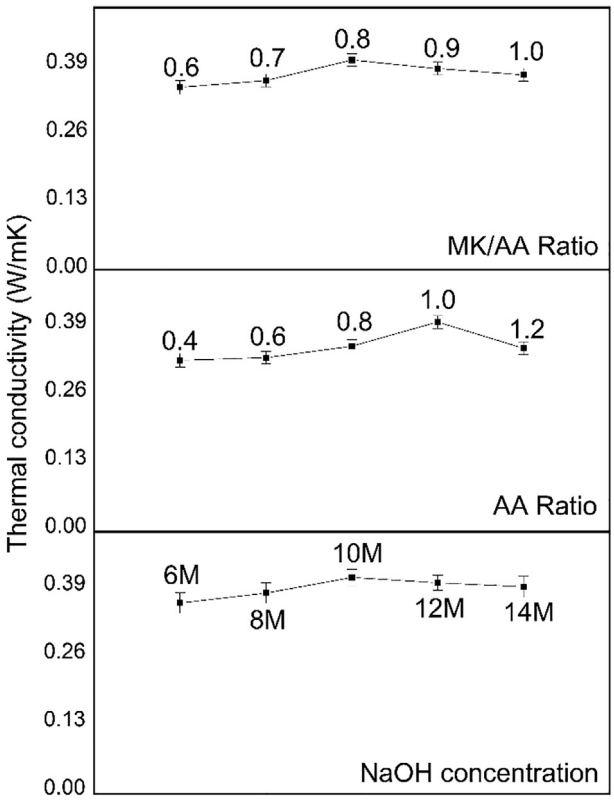


**Fig. 5.** Thermal conductivity values of metakaolin geopolymer.

**Table 4**
Correlation coefficient ($R^2$) of TC versus compressive strength, bulk density, and porosity.

| Parameters | λ versus Compressive Strength | λ versus Bulk Density | λ versus Porosity |
|---|---|---|---|
| NaOH concentration | 0.7244 | 0.861 | 0.8453 |
| AA ratio | 0.7445 | −0.124 | 0.4600 |
| MK/AA ratio | 0.7900 | 0.894 | 0.9834 |

used as a measure of the strength dependency between two variables. The nearer the correlation coefficient to value of 1.0 indicates a strong functional relationship. The λ had a strong relationship with porosity and bulk density which varied most substantially with the MK/AA ratio. The solid and liquid contents in geopolymer mixture determined the efficiency of dissolution and formation of dense matrix. This statement was supported by Rickard [56] and Duxson et al. [53] who stated that liquid content was a substantial part of the mixture and will definitely influence properties such as porosity and density. Pore formation reduced the λ due to extremely low λ of air in the enclosed pores which contributed to an overall lower λ value [57]. It was observed that, regardless of the mixing parameter, the λ value would not differ much if the porosity was similar.

### 3.2. Metakaolin geopolymer foam

#### 3.2.1. Bulk density and porosity

Fig. 6 shows the bulk density and porosity of metakaolin geopolymer foam. At fixed $H_2O_2$ content, increasing surfactant content decreased the bulk density and increased porosity. Besides as pore stabilizer, surfactant also acted as air-entraining admixture [16] creating pores in the matrix and reducing the bulk density. At the same time, at fixed surfactant content, bulk density reduced, while porosity increased with increasing foaming agent content. This was expected and well-agreed by several researchers [15,58]. The bulk density and porosity were in the range of 471–1212 kg/m$^3$ and 36–86%, respectively. The oxygen gas released as a result of $H_2O_2$ decomposition trapped within paste and expanded to generate more voids and subsequently reduced bulk density.

The decrement of bulk density was more obvious at low $H_2O_2$ content (<0.75 wt%) and slowed down at higher $H_2O_2$ content (>0.75 wt%), regardless of the surfactant content. A similar observation was noticed for porosity whereby porosity increased to a greater extent at low $H_2O_2$ content and a slower extent at higher $H_2O_2$ content. Nevertheless, it was more prominent at lower surfactant content (<2 wt%). This implied that the extent of pore formation decreased at higher $H_2O_2$ content. A high amount of foaming agent would have generated high amount of pores in geopolymer matrix which finally merged and collapsed. On due course, the bulk density and porosity did not change significantly at high $H_2O_2$ content. Besides, the variation in the bulk density and porosity was governed mainly by the $H_2O_2$ content rather than surfactant content. This was because $H_2O_2$ had more tendency to collapse than surfactant. Based on Ashby et al. [59], surfactant entrained air (mainly $N_2$) which was less permeable than $O_2$ produced by $H_2O_2$.

#### 3.2.2. Compressive strength

The metakaolin geopolymer foam demonstrated a downward compressive strength trend with increasing foaming agent and surfactant contents (Fig. 7a). The compressive strength was in the range of 0.4–6.0 MPa after 28 days with a density range of 471–1212 kg/m$^3$. The reduction of compressive strength was due to the increased pores generated by the decomposition of $H_2O_2$. The pores acted as the stress concentration point and prone to failure when load is applied. Thus, the geopolymer foam tended to deteriorate easily with increasing porosity. Besides, the compressive strength was also influenced by the pore size which will be discussed in Section 3.2.4. Complied with the bulk density and porosity results (Fig. 6), the compressive strength decreased at a faster rate at lower $H_2O_2$ (<0.75 wt%) and surfactant content (<2 wt%) due to greater rate of pore formation. The compressive strength development was influenced more significantly by $H_2O_2$ content compared to surfactant content, as mentioned earlier, due to the greater variation in porosity and density with changing $H_2O_2$ content. The observation was contrary to that reported by Samson et al. [20] who stated that compressive strength was sensitive to the surfactant content.

Geopolymer foam usually possessed extremely low compressive strength. The addition of surfactant enhanced the compressive strength of geopolymer foam. Higher compressive strength was obtained in this study compared to those geopolymer foams without surfactant. For instance, Novais et al. [6] reported compressive strength of 0.05–0.38 MPa for $H_2O_2$-foamed fly ash geopolymer with a similar density range (500–1300 kg/m$^3$). Compressive

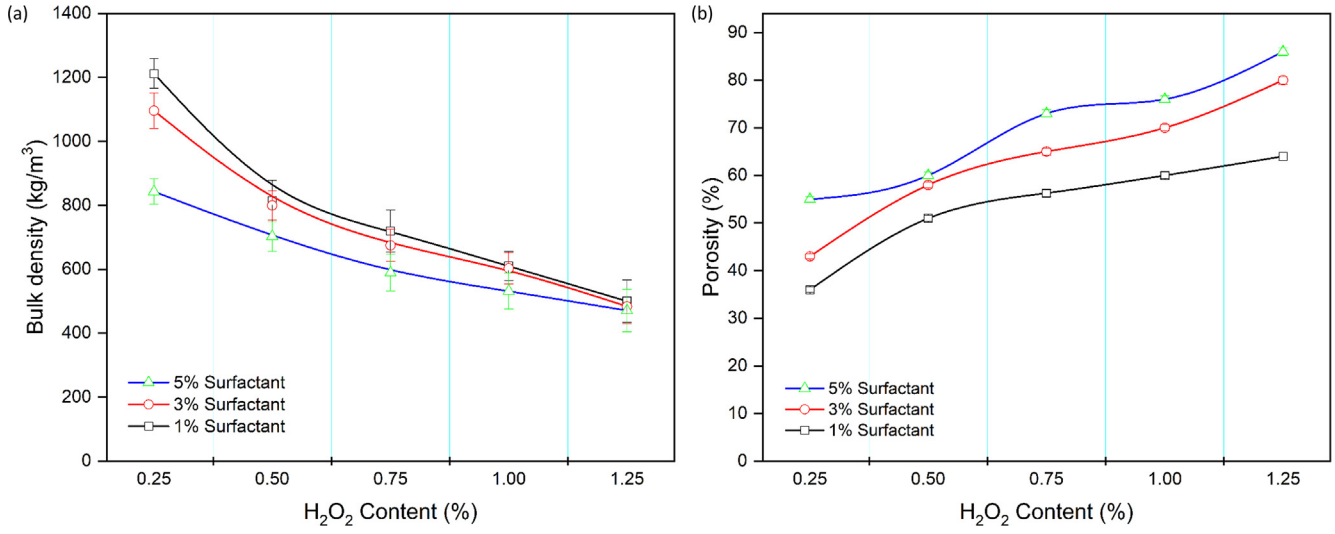


**Fig. 6.** (a) Bulk density and (b) porosity of metakaolin geopolymer foam.

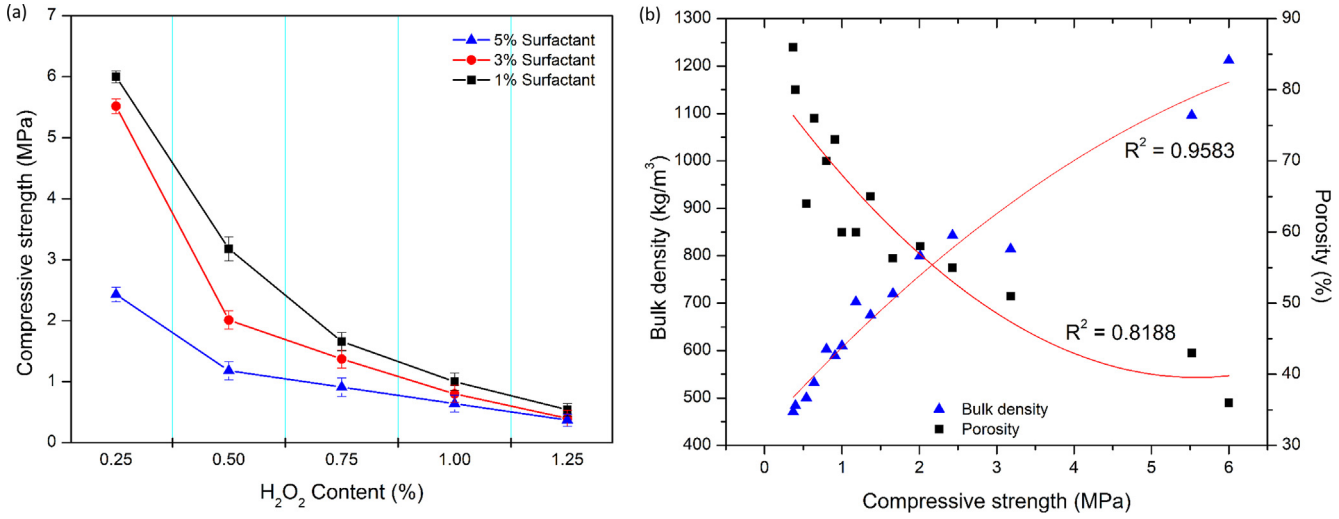


**Fig. 7.** (a) Compressive strength and (b) correlation curve of geopolymer foam.

strength of 0.26–10 MPa at density 440–1100 kg/m$^3$ was also reported for metakaolin-fly ash geopolymer foam. Even with a similar density range, the compressive strength reported was higher than that obtained in this study as the porosity was lower (52.3–80.9%) [60]. Feng et al. [9] reported compressive strength of 0.38–0.60 MPa for fly ash geopolymer foam. On the other hand, a low compressive strength of 0.42–1.59 MPa has been concluded by Hajimohammadi et al. [61] for fly ash geopolymer foamed with aluminium powder. As compared to PC foam [62], similar compressive strength (2.5–6.5 MPa) and density (860–1245 kg/m$^3$) were obtained.

In addition, the compressive strength of geopolymer foam in this study was higher than those reported by Bai & Colombo [63] (0.3–4.4 MPa) who also produced metakaolin geopolymer foam with $H_2O_2$ and surfactant (Tween 80). The higher compressive strength recorded in this study was most probably due to the higher bulk density. According to Samson et al. [20], the highest achievable compressive strength of metakaolin geopolymer foamed with $H_2O_2$ and surfactant was 3.34 MPa. With a similar density range, Petlitckaia & Poulesquen [64] obtained similar compressive strength for metakaolin geopolymer foamed with $H_2O_2$ and cetyltrimethyl ammonium bromide (CTAB) as surfactant. Based on their study, geopolymers foam added with CTAB as cathionic surfactant had better mechanical performance and pore stabilising ability than non-ionic surfactant (e.g. Tween 80). However, a contrary conclusion was observed in this study. Moreover, Korat & Ducman [58] reported higher compressive strength of 2.6–12.2 MPa for fly ash geopolymer foamed using $H_2O_2$ and SDS surfactant which was most probably owing to high density (580–1340 kg/m$^3$).

Based on Fig. 7b, compressive strength had a strong relationship with bulk density and porosity with $R^2$ = 0.9583 and $R^2$ = 0.8188, respectively. The higher bulk density and lower porosity contributed to higher compressive strength and vice versa. The density and formation of pores or voids determined the final strength of compressive strength [65].

### 3.2.3. Thermal conductivity (λ)

The incorporation of foaming agent further reduced the λ of the non-foamed geopolymer. The geopolymer foams showed obvious decrease in the λ value (0.11–0.30 W/mK) (Fig. 8) compared to non-foamed geopolymer (0.40 W/mK). This was due to the presence of air voids in the geopolymer matrix generated by the foaming agent in the mixture. The greater the porosity (Fig. 6b), the lower the λ value. Based on correlation curve in Fig. 9, thermal conductivity of geopolymer foam had stronger relationship with bulk density ($R^2$ = 0.9606) and porosity ($R^2$ = 0.9583) compared to compressive strength ($R^2$ = 0.8060). The highly porous structure acted as an effective barrier against the heat flow within the geopolymer network and hence leading to lower λ [27]. The effect of $H_2O_2$ content was more prominent in reducing the λ value compared to surfactant content as higher $H_2O_2$ content was associated with increased foam-ability and greater pore formation.

The λ values were comparable with those obtained by Kamseu et al. [24] and Novais et al. [6] for foamed metakaolin geopolymer (0.15–0.40 W/mK) and foamed biomass fly ash geopolymer (0.005–0.39 W/mK), respectively. With similar density range (600–1200 kg/m$^3$), Aguilar et al. [66] reported higher λ values (0.49–1.22 W/mK) for metakaolin geopolymer foam. Table 5 summarises the bulk density, porosity, compressive strength and thermal conductivity of various types of geopolymer foams and lightweight insulated materials. As compared to other commercially available thermal-insulated materials such as wool and expanded polystyrene (EPS), the thermal conductivity reported in this study was slightly higher. However, considering the properties of geopolymers, insulating material based on geopolymer is a potential candidate. With the bulk density, compressive strength

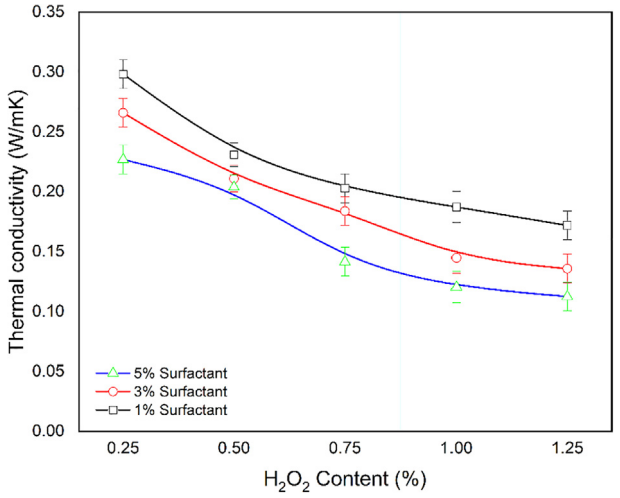


**Fig. 8.** Thermal conductivity of metakaolin geopolymer foam.

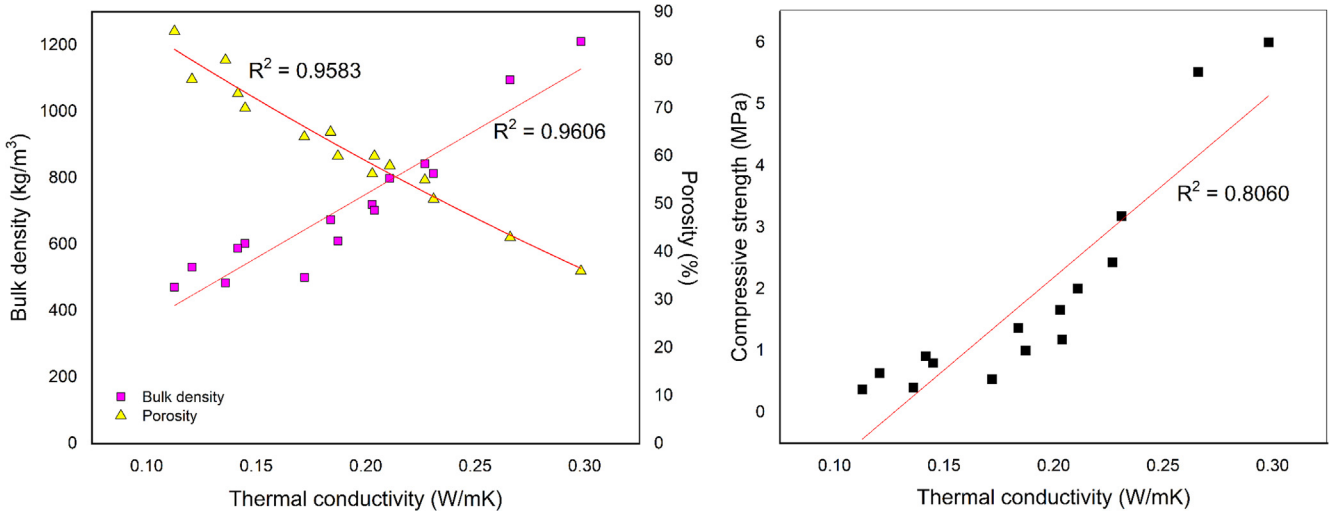


**Fig. 9.** Correlation between thermal conductivity with bulk density, porosity, and compressive strength.

and thermal conductivity obtained, the metakaolin geopolymer foam could be regarded as Class II lightweight concrete for structural and insulating purposes according to the RILEM [18].

### 3.2.4. Microstructural analysis

Fig. 10 reveals the microstructures of metakaolin geopolymer foam with varying amounts of hydrogen peroxide and surfactant. The average pore diameter was also labelled in the SEM micrographs. Fig. 11 presents the pore size distribution of geopolymer foam and the relationship between pore diameter and compressive strength. The pore size of geopolymer foam with $H_2O_2$ content of 1.25 wt% could not be measured due to connected pores.

In overall, geopolymer foam presented loose and porous structure distributed homogeneously throughout the matrix. The average pore diameter increased with $H_2O_2$ and surfactant contents (Fig. 10). At low $H_2O_2$ (0.25 wt%), all pores were spherical and smaller than 300 μm (Fig. 11). The narrow range of pore size helped in achieving greater compressive strength (Fig. 7). A gradual increase in the coarser pores was observed with increasing $H_2O_2$ content. The decrease in the smaller pores and the increase in large pores were also observed with increasing surfactant content. The pores became slightly oval in shape. The probability of forming larger pores was facilitated with high $H_2O_2$ and surfactant contents. On due course, the mechanical strength decreased (Fig. 7a). The change of the geometric shape of pores with increasing $H_2O_2$ content was supported by Lynch et al. [71] and Vaou & Panias [70]. In addition, referring to Fig. 10, the extent of pore size enlargement was more obvious with increasing $H_2O_2$ content compared to increasing surfactant content. This verified the observation above that $H_2O_2$ was more prominent in affecting the physical and mechanical properties. A large amount of pore formed in the geopolymer sample also indicated low binding materials to contribute to strength development [72].

According to Nguyen et al. [17], a porous structure comprised of 3 types of pores, namely the gel pores (<10 nm), capillary pores (10 nm–10 μm) and air voids (>10 μm). In this study, the pores with size ranged up to 500 μm (Fig. 11) were categorised as the air voids. On the other hand, pores with a radius greater than 50 μm were referred to as macro-pores [73]. Both air voids and macro-pores were influential on the mechanical strength of geopolymer. Based on Fig. 11d, increasing average pore diameter significantly reduced the compressive strength of geopolymer foam with $R^2$ = 0.8077.

High $H_2O_2$ (>1.0 wt%) caused some pores to collapse and/or coalesce forming large and connected pores. This phenomenon worsened with increasing surfactant content. As discussed earlier, the decomposition of $H_2O_2$ under alkali media released $O_2$ gas in the geopolymer matrix. When the $O_2$ gas formed exceeding threshold, the pores expanded and increased in size. The pore wall of some pores might get thinner and tend to burst and merge. Pore coalescence occurred when the pores become overly large, collapse and connected [16]. Some pores may move upward to the surface

**Table 5**
Summary of physical and mechanical properties and thermal conductivity of thermal-insulated materials.

| Category | Aluminosilicate | Foam types/Filler | Bulk density kg/m³ | Total porosity % | Compressive strength MPa | Thermal conductivity W/mK | Reference |
|---|---|---|---|---|---|---|---|
| Geopolymer | Metakaolin | $H_2O_2$[1] | 470–1210 | 36–86 | 0.37–6.00 | 0.11–0.30 | This work |
| Geopolymer | Biomass fly ash | $H_2O_2$ | 560–1200 | NA | 0.12–0.42 | 0.005–0.39 | [6] |
| Geopolymer | Metakaolin | $H_2O_2$ | 300–580 | 74–87 | 0.30–4.40 | 0.09 –0.16 | [63] |
| Geopolymer | Metakaolin | $H_2O_2$ | 400–510 | 62–81 | 2.19–3.11 | NA | [67] |
| Geopolymer | Fly ash | $H_2O_2$ | 240–340 | 79–81 | 0.60–0.38 | 0.09–0.07 | [9] |
| Geopolymer | Metakaolin | Polystyrene | 100–400 | NA | 3.20–4.20 | 0.04–0.08 | [68] |
| Geopolymer | Metakaolin + Slag | $H_2O_2$[1] | 264–480 | NA | 0.53–3.34 | 0.084–0.139 | [20] |
| Geopolymer | Metakaolin + Fly ash | $H_2O_2$ | 440–1100 | 52–81 | 0.26–10.00 | 0.08–0.22 | [60] |
| Geopolymer | Fly Ash | $H_2O_2$[1] | 580–1340 | NA | 2.60–12.20 | NA | [58] |
| PC foam | NA | Preformed Foam | 360–1400 | NA | 1.00–10.00 | 0.15–0.60 | [69] |
| Extruded polystyrene (EPS) | NA | NA | 20–80 | NA | 0.10–0.70 | 0.03–0.04 | [70] |
| Expanded clay | NA | NA | 260–500 | NA | NA | 0.09–0.16 | [70] |
| Glass wool | NA | NA | 100–130 | NA | 0.03–0.05 | 0.16 | [70] |

*NA – not available.
[1] With surfactant.

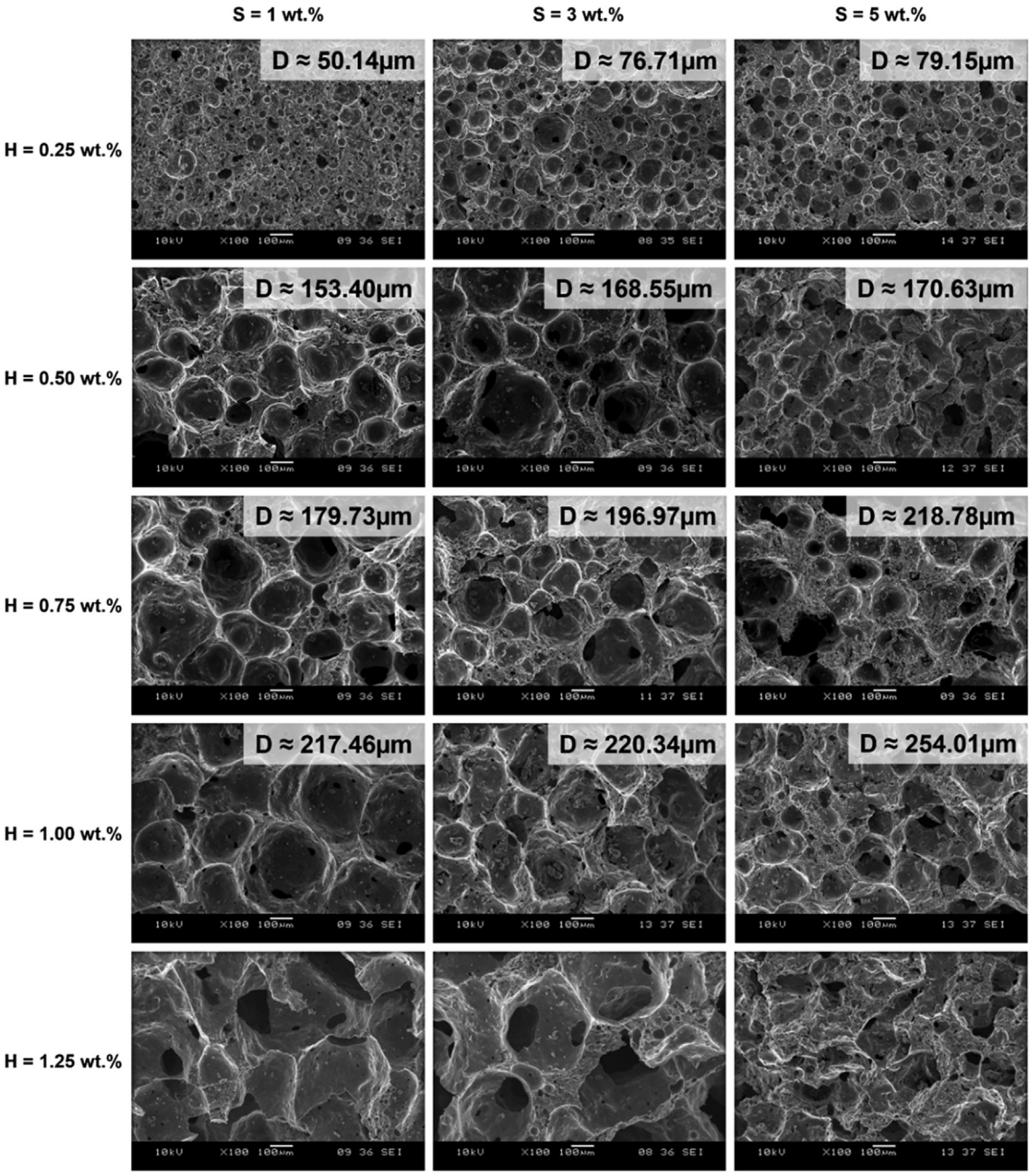


**Fig. 10.** SEM micrographs of metakaolin geopolymer foam with varying surfactant (S) and $H_2O_2$ (H) contents. D represents the average pore diameter.

and escape. This was believed leading to the slow-down growth of bulk density and porosity (Fig. 6).

Referring to Fig. 10, the surfactant improved the stability of pores at low $H_2O_2$ content (<0.75 wt%). The surfactant avoided excess coalescence of pores [20]. This was evidenced by the small changes in the average pore diameter (Fig. 10). The use of surfactant in conjunction with low $H_2O_2$ content produced a more homogeneous pore structure. Nevertheless, the pore stabilizing ability abated with increasing $H_2O_2$ content (>0.75 wt%). As refer to Eq. (1), water was released during the decomposition of $H_2O_2$ in alkali media. This reduced the viscosity of geopolymer mixture which subsequently affecting the stability of pores. Wet mixes restricted the pore stabilizing and/or air entrainment in proper size and distribution.

The pore connectivity had a significant impact on heat transfer [8]. As mentioned above, heat transfer was controlled by the tortuosity of the matrix. Highly porous structure reduced the λ value. At low $H_2O_2$ content, despite having closed and fine pores, the porosity was lesser. Thus, the λ value was higher [22]. It was supposed that the λ value decreased linearly with increasing $H_2O_2$ content. However, the pores became interconnected at high $H_2O_2$ content and did not cause an extensive reduction in the λ value as shown in Fig. 8.

### 3.2.5. XRD analysis

Fig. 12 illustrates the XRD diffractogram of metakaolin and metakaolin geopolymer. Metakaolin showed a wide diffraction hump between 18° and 25° 2θ attributed to the amorphous structure of metakaolin [2]. Kaolinite (K) and quartz (Q) peaks were detected in the metakaolin. The presence of kaolinite in metakaolin indicated incomplete calcination of kaolin.

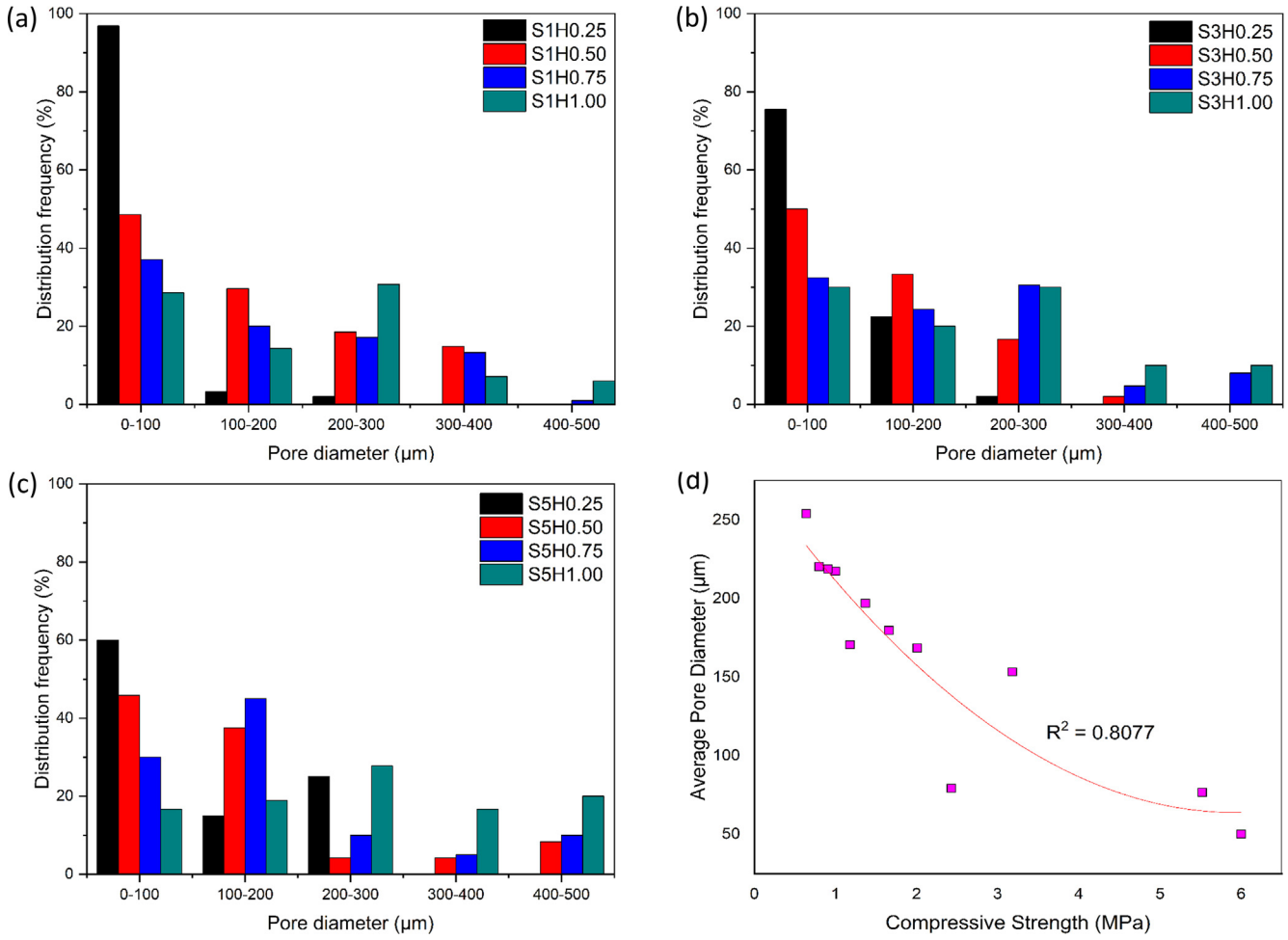


**Fig. 11.** Pore size distribution of the geopolymer foam (a–c) and the correlation between average pore diameter and compressive strength (d) (H – $H_2O_2$ and S – Surfactant).

Alkali activation of metakaolin shifted the diffuse hump to a higher angle (20°–35° 2θ) which represented the primary binder phase of geopolymer [74]. The dominant amorphous gel phase represented the sodium aluminosilicate gel (N-A-S-H) which was the main factor contributing to the mechanical properties of metakaolin geopolymer. Most of the kaolinite peaks disappeared due to the dissolution in alkali solution. Kaolinite peak at 19.8° was still present in the metakaolin geopolymer due to the presence of unreacted metakaolin particles in the geopolymer matrix. In addition, quartz peak can still be found in the metakaolin geopolymer after the geopolymerisation reaction confirmed its insolubility in the reaction [75]. The phase analysis of geopolymer foam was not performed as the hydrogen peroxide and surfactant did not cause any changes to the XRD pattern of geopolymer.

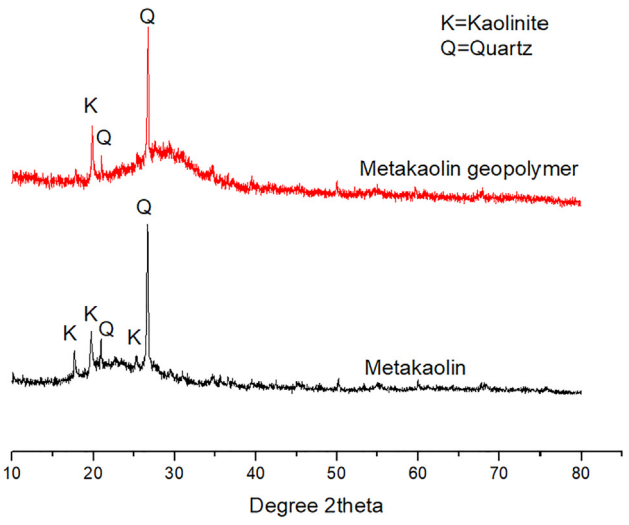


**Fig. 12.** XRD diffractogram of metakaolin and metakaolin geopolymer.

## 4. Conclusions

This paper investigates mainly the effect of mixing parameters, foaming agent and surfactant on the physical and mechanical properties as well as the thermal conductivity of metakaolin geopolymer. The pore characteristic of the foamed geopolymer was also studied. Optimized metakaolin geopolymers had a compressive strength of 33 MPa after 28 days prepared using NaOH concentration of 10 M, AA ratio of 1.0 and MK/AA ratio of 0.80. The strength determining factor was: AA ratio > MK/AA ratio > NaOH concentration. MK/AA ratio had the most significant effect on the thermal conductivity due to its greater effect on the porosity level of geopolymer.

Incorporation of $H_2O_2$ and surfactant reduced the compressive strength (0.4–6.0 MPa), bulk density (471–1212 kg/m$^3$) and thermal conductivity (0.11–0.30 W/mK), while increased the porosity (36–86%). Both $H_2O_2$ and surfactant contributed to pore formation.

Apart from being a pore stabilizer, the surfactant acted as an air-entraining admixture. The combination of $H_2O_2$ and surfactant produced narrower pore size and distribution compared to using the foaming agent alone. The increasing $H_2O_2$ dosage led to greater change in the pore diameter and distribution compared to increasing surfactant. The effect of surfactant was more obvious at low $H_2O_2$ content and the pore stabilizing effect lessened at high $H_2O_2$ content. This happened due to the reduced viscosity at high $H_2O_2$ content as a result of $H_2O_2$ decomposition. Hence, the viscosity of geopolymer paste might affect the effectiveness of surfactant in maintaining the pores. The characteristic of pore in the matrix either closed-pore or open pores affected the effective thermal transfer and thus the thermal conductivity.

## CRediT authorship contribution statement

**Nur Ain Jaya:** Methodology, Investigation, Writing - original draft. **Liew Yun-Ming:** Conceptualization, Writing - review & editing, Supervision. **Heah Cheng-Yong:** Visualization. **Mohd Mustafa Al Bakri Abdullah:** Resources. **Kamarudin Hussin:** Resources.

## Declaration of Competing Interest

The authors declare that they have no known competing financial interests or personal relationships that could have appeared to influence the work reported in this paper.

## Acknowledgments

The authors earnestly deliver their gratitude to the funding provided by Fundamental Research Grant Scheme (FRGS/1/2015/TK05/UNIMAP/02/2) sponsored by the Ministry of Education Malaysia and "Partnership for Research in Geopolymer Concrete" (H2020-MSCA-RISE-2015-689857-PRIGeoC) sponsored by the European Union.

## References

[1] C.D. Atiş et al., Very high strength (120 MPa) class F fly ash geopolymer mortar activated at different NaOH amount, heat curing temperature and heat curing duration, Constr. Build. Mater. 96 (2015) 673–678.
[2] L. Chen et al., Preparation and properties of alkali activated metakaolin-based geopolymer, Materials 9 (9) (2016) 767.
[3] T. Luukkonen et al., One-part alkali-activated materials: a review, Cem. Concr. Res. 103 (2018) 21–34.
[4] S. Yaseri et al., The role of synthesis parameters on the workability, setting and strength properties of binary binder based geopolymer paste, Constr. Build. Mater. 157 (2017) 534–545.
[5] N. Ye et al., Synthesis and strength optimization of one-part geopolymer based on red mud, Constr. Build. Mater. 111 (2016) 317–325.
[6] R.M. Novais et al., Porous biomass fly ash-based geopolymers with tailored thermal conductivity, J. Cleaner Prod. 119 (2016) 99–107.
[7] Subaer, A. van Riessen, Thermo-mechanical and microstructural characterisation of sodium-poly(sialate-siloxo) (Na-PSS) geopolymers, J. Mater. Sci. 42 (2007) 3117–3123.
[8] R.T.T. Fongang et al., Cleaner production of the lightweight insulating composites: microstructure, pore network and thermal conductivity, Energy Build. 107 (2015) 113–122.
[9] J. Feng et al., Development of porous fly ash-based geopolymer with low thermal conductivity, Mater. Des. (1980–2015) 65 (2015) 529–533.
[10] J.G. Sanjayan et al., Physical and mechanical properties of lightweight aerated geopolymer, Constr. Build. Mater. 79 (2015) 236–244.
[11] J. Henon et al., Potassium geopolymer foams made with silica fume pore forming agent for thermal insulation, J. Porous Mater. 20 (1) (2012) 37–46.
[12] J. Wu et al., Preparation and characterization of ultra-lightweight foamed geopolymer (UFG) based on fly ash-metakaolin blends, Constr. Build. Mater. 168 (2018) 771–779.
[13] N. Boke et al., New synthesis method for the production of coal fly ash-based foamed geopolymers, Constr. Build. Mater. 75 (2015) 189–199.
[14] Z. Abdollahnejad et al., Mix design, properties and cost analysis of fly ash-based geopolymer foam, Constr. Build. Mater. 80 (2015) 18–30.
[15] Z. Zhang et al., Mechanical, thermal insulation, thermal resistance and acoustic absorption properties of geopolymer foam concrete, Cem. Concr. Compos. 62 (2015) 97–105.
[16] G. Masi et al., A comparison between different foaming methods for the synthesis of lightweight geopolymers, Ceram. Int. 40 (2014) 13891–13902.
[17] T.T. Nguyen et al., A micromechanical investigation for the effects of pore size and its distribution on geopolymer foam concrete under uniaxial compression, Eng. Fract. Mech. 209 (2019) 228–244.
[18] A.C. Institute, Building Code Requirements for Structural Concrete (ACI 318M–11) and Commentary, Farmington Hills Michigan, 2011.
[19] F. Xu et al., Pore structure analysis and properties evaluations of fly ash-based geopolymer foams by chemical foaming method, Ceram. Int. 44 (2018) 19989–19997.
[20] G. Samson, M. Cyr, X.X. Gao, Thermomechanical performance of blended metakaolin-GGBS alkali-activated foam concrete, Constr. Build. Mater. 157 (2017) 982–993.
[21] V. Medri et al., Effect of metallic Si addition on polymerization degree of in situ foamed alkali-aluminosilicates, Ceram. Int. 39 (7) (2013) 7657–7668.
[22] Z. Zhang et al., Geopolymer foam concrete: an emerging material for sustainable construction, Constr. Build. Mater. 56 (2014) 113–127.
[23] V. Ducman, L. Korat, Characterization of geopolymer fly-ash based foams obtained with the addition of Al powder or $H_2O_2$ as foaming agents, Mater. Charact. 113 (2016) 207–213.
[24] E. Kamseu et al., Bulk composition and microstructure dependence of effective thermal conductivity of porous inorganic polymer cements, J. Eur. Ceram. Soc. 32 (8) (2012) 1593–1603.
[25] D.M.A. Huiskes et al., Design and performance evaluation of ultra-lightweight geopolymer concrete, Mater. Des. 89 (2016) 516–526.
[26] Z. Liu et al., Effect of $SiO_2/Na_2O$ mole ratio on the properties of foam geopolymers fabricated from circulating fluidized bed fly ash, Int. J. Miner. Metall. Mater. 21 (6) (2014) 620–626.
[27] A. Hajimohammadi et al., Alkali activated slag foams: the effect of the alkali reaction on foam characteristics, J. Cleaner Prod. 147 (2017) 330–339.
[28] Y. Cui et al., Effect of calcium stearate based foam stabilizer on pore characteristics and thermal conductivity of geopolymer foam material, J. Build. Eng. 20 (2018) 21–29.
[29] I. Beghoura, J. Castro-Gomes, Design of alkali-activated aluminium powder foamed materials for precursors with different particle sizes, Constr. Build. Mater. 224 (2019) 682–690.
[30] Q. Wan, F. Rao, S. Song, Reexamining calcination of kaolinite for the synthesis of metakaolin geopolymers – roles of dehydroxylation and recrystallization, J. Non-Cryst. Solids 460 (2017) 74–80.
[31] T. Bakharev, Geopolymeric materials prepared using Class F f ly ash and elevated temperature curing, Cem. Concr. Res. 35 (2005) 1224–1232.
[32] H.Y. Fen et al., Effect of activator and curing mode on fly ash-based geopolymers, J. Wuhan Univ. Technol. 24 (2009) 711–715.
[33] P. Rożek, M. Król, W. Mozgawa, Spectroscopic studies of fly ash-based geopolymers, Spectrochim. Acta Part A: Mol. Biomol. Spectrosc. 198 (2018) 283–289.
[34] C. Tippayasam et al., Potassium alkali concentration and heat treatment affected metakaolin-based geopolymer, Constr. Build. Mater. 104 (2016) 293–297.
[35] E. Papa et al., Zeolite-geopolymer composite materials: Production and characterization, J. Cleaner Prod. 171 (2018) 76–84.
[36] P. Rożek, M. Król, W. Mozgawa, Geopolymer-zeolite composites: a review, J. Cleaner Prod. 230 (2019) 557–579.
[37] G. Görhan, G. Kürklü, The influence of the NaOH solution on the properties of the fly ash-based geopolymer mortar cured at different temperatures, Compos. B: Eng. 58 (2014) 371–377.
[38] H.Y. Leong et al., The effect of different $Na_2O$ and $K_2O$ ratios of alkali activator on compressive strength of fly ash based-geopolymer, Constr. Build. Mater. 106 (2016) 500–511.
[39] C. Kuenzel et al., Influence of metakaolin characteristics on the mechanical properties of geopolymers, Appl. Clay Sci. 83–84 (2013) 308–314.
[40] D. Yan et al., Correlating the elastic properties of metakaolin-based geopolymer with its composition, Mater. Des. 95 (2016) 306–318.
[41] M. Glid et al., Alkaline activation of metakaolinite-silica mixtures: role of dissolved silica concentration on the formation of geopolymers, Ceram. Int. 43 (15) (2017) 12641–12650.
[42] H. Wang, H. Li, F. Yan, Synthesis and mechanical properties of metakaolinite-based geopolymer, Colloids Surf., A 268 (1–3) (2005) 1–6.
[43] Q. Wan et al., Geopolymerization reaction, microstructure and simulation of metakaolin-based geopolymers at extended Si/Al ratios, Cem. Concr. Compos. 79 (2017) 45–52.
[44] F. Pelisser et al., Micromechanical characterization of metakaolin-based geopolymers, Constr. Build. Mater. 49 (2013) 547–553.
[45] A. Poowancum, S. Horpibulsuk, Development of low cost geopolymers from calcined sedimentary clay, in: A.F. Karen Scrivener (Ed.), Calcined Clays for Sustainable Concrete: Proceedings of the 1st International Conference on Calcined Clays for Sustainable Concrete, Springer, 2015.
[46] M. Ibrahim et al., Effect of alkaline activators and binder content on the properties of natural pozzolan-based alkali activated concrete, Constr. Build. Mater. 147 (2017) 648–660.
[47] M. Rowles, B. O'Connor, Chemical optimisation of the compressive strength of aluminosilicate geopolymers synthesized by sodium silicate activation of metakaolinite, J. Mater. Chem. 13 (2003) 1161–1165.
[48] T.S. Yun et al., Evaluation of thermal conductivity for thermally insulated concretes, Energy Build. 61 (2013) 125–132.

[49] C. Kuenzel et al., Production of nepheline/quartz ceramics from geopolymer mortars, J. Eur. Ceram. Soc. 33 (2013) 251–258.
[50] P. He, D. Jia, S. Wang, Microstructure and integrity of leucite ceramic derived from potassium-based geopolymer precursor, J. Eur. Ceram. Soc. 33 (2013) 689–698.
[51] Z. Pan et al., Damping and microstructure of fly ash-based geopolymers, J. Mater. Sci. 48 (8) (2012) 3128–3137.
[52] M. Albitar et al., Durability evaluation of geopolymer and conventional concretes, Constr. Build. Mater. 136 (2017) 374–385.
[53] P. Duxson, G.C. Lukey, J.S.J.V. Deventer, Thermal conductivity of metakaolin geopolymers used as a first approximation for determining gel interconnectivity, Ind. Eng. Chem. Res. 45 (2006) 7781–7788.
[54] E. Kamseu et al., Insulating behavior of metakaolin-based geopolymer materials assess with heat flux meter and laser flash techniques, J. Therm. Anal. Calorim. 108 (2012) 1189–1199.
[55] M.A. Villaquiran-Caicedo et al., Thermal properties of novel binary geopolymers based on metakaolin and alternative silica sources, Appl. Clay Sci. 118 (2015) 276–282.
[56] W.D.A. Rickard, Assessing the Suitability of Fly Ash Geopolymers for High Temperature Applications, in Department of Imaging and Applied Physics, Curtin University, 2012.
[57] A. Wongsa et al., Mechanical and thermal properties of lightweight geopolymer mortar incorporating crumb rubber, J. Cleaner Prod. 195 (2018) 1069–1080.
[58] L. Korat, V. Ducman, The influence of the stabilizing agent SDS on porosity development in alkali-activated fly-ash based foams, Cem. Concr. Compos. 80 (2017) 168–174.
[59] M. Ashby et al., Metal Foams: A Design Guide, first ed., Butterworth-Heinemann, 2000.
[60] R.M. Novais et al., Influence of blowing agent on the fresh- and hardened-state properties of lightweight geopolymers, Mater. Des. 108 (2016) 551–559.
[61] A. Hajimohammadi et al., Regulating the chemical foaming reaction to control the porosity of geopolymer foams, Mater. Des. 120 (2017) 255–265.
[62] N. Vinith Kumar, C. Arunkumar, S. Srinivasa Senthil, Experimental study on mechanical and thermal behavior of foamed concrete, Mater. Today:. Proc. 5 (2) (2018) 8753–8760.
[63] C. Bai, P. Colombo, High-porosity geopolymer membrane supports by peroxide route with the addition of egg white as surfactant, Ceram. Int. 43 (2) (2017) 2267–2273.
[64] S. Petlitckaia, A. Poulesquen, Design of lightweight metakaolin based geopolymer foamed with hydrogen peroxide, Ceram. Int. 45 (2019) 1322–1330.
[65] S. Yan et al., Green synthesis of high porosity waste gangue microsphere/geopolymer composite foams via hydrogen peroxide modification, J. Cleaner Prod. 227 (2019) 483–494.
[66] R.A. Aguilar, O.B. Diaz, J.I.E. Garcia, Lightweight concretes of activated metakaolin-fly ash binders, with blast furnace slag aggregates, Constr. Build. Mater. 24 (7) (2010) 1166–1175.
[67] C. Bai et al., High strength metakaolin-based geopolymer foams with variable macroporous structure, J. Eur. Ceram. Soc. 36 (16) (2016) 4243–4249.
[68] P. Duan et al., Novel thermal insulating and lightweight composites from metakaolin geopolymer and polystyrene particles, Ceram. Int. 43 (2017) 5115–5120.
[69] E.K.K. Nambiar, K. Ramamurthy, Influence of filler type on the properties of foam concrete, Cem. Concr. Compos. 28 (5) (2006) 475–480.
[70] V. Vaou, D. Panias, Thermal insulating foamy geopolymers from perlite, Miner. Eng. 23 (2010) 1146–1151.
[71] J.L.V. Lynch et al., Preparation, characterization, and determination of mechanical and thermal stability of natural zeolite-based foamed geopolymers, Constr. Build. Mater. 172 (2018) 448–456.
[72] K.K. Schiller, Strength of porous materials, Cem. Concr. Res. 1 (4) (1971) 419–422.
[73] N. Narayanan, K. Ramamurthy, Structure and properties of aerated concrete: a review, Cem. Concr. Compos. 22 (2000) 321–329.
[74] H. Rahier et al., Reaction mechanism, kinetics and high temperature transformations of geopolymers, J. Mater. Sci. 42 (2007) 2982–2996.
[75] Q. Wan et al., Combination formation in the reinforcement of metakaolin geopolymers with quartz sand, Cem. Concr. Compos. 80 (2017) 115–122.